

*H Bonds in Carbohydrates***Direct Detection of Inter-residue Hydrogen Bonds in Polysaccharides by Single-Molecule Force Spectroscopy*****Qingmin Zhang, Justyna Jaroniec, Gwangrog Lee, and Piotr E. Marszalek**

Hydrogen bonds (H bonds) play important roles in determining the structure and function of biopolymers. For example, they are responsible for base pairing in nucleic acids, they contribute to the stability of proteins folds, and they control molecular recognition among proteins, DNA, and carbohydrates.^[1] Polysaccharides, because of their abundance of hydroxy groups and oxygen atoms, are prone to form extensive networks of intra- and intermolecular hydrogen bonds.^[2] The ubiquitous polysaccharide cellulose extensively

[*] Dr. Q. Zhang, J. Jaroniec, G. Lee, Prof. P. E. Marszalek
Center for Biologically Inspired Materials and Material Systems
Department of Mechanical Engineering and Materials Science
Duke University
Durham, NC 27708 (USA)
Fax: (+1) 919-660-8963
E-mail: pemar@duke.edu

[**] This work was supported by a grant from the National Science Foundation and by Duke University funds to P.E.M. We thank Prof. Yasuhiro Takahashi of Osaka University, Japan for a sample of amylose triacetate.



Supporting information for this article is available on the WWW under <http://www.angewandte.org> or from the author.

exploits intra- and intermolecular H bonds to form microfibrils that provide impressive mechanical strength to the cell wall in plants.^[3] The existence of specific H bonds in biopolymers, including polysaccharides, is not always easy to detect directly. More typically H bonds are deduced based on the positions of putative H-bond donor and acceptor atoms, which are determined experimentally by X-ray/neutron diffraction or NMR spectroscopy,^[2–5] or they are identified by computer modeling.^[6,7] In solutions H bonds may be disturbed or eliminated altogether because their donors and acceptors may engage intermittently in hydrogen bonding with solvent molecules. Therefore, the existence of H bonds in a liquid phase is rather difficult to establish experimentally.

Herein we report a new approach to directly examine the propensity of polysaccharides to form inter-residue H bonds under various solvent conditions. This method involves single-molecule force spectroscopy^[8,9] to measure the effect of H bonds on the elasticity of individual polysaccharide chains using the atomic force microscope (AFM). This technique was, for example, used to determine the role of water bridges in the helical structure of poly(ethyleneglycol)^[9] and to measure the effect of H bonds on the elasticity of a modular protein, titin.^[10]

In force spectroscopy, single polymer chains are attached at their extremities to a substrate and the AFM tip and are stretched vertically in solution to determine their force–extension relationships (force spectrograms). The force spectrogram of a simple polymer is typically described in the context of the entropic elasticity of the freely jointed chain (FJC) model.^[11] However, the majority of the polysaccharides studied so far by AFM do not behave as FJCs.^[8,12–14] Their force spectrograms display various enthalpic features that are mechanical fingerprints of force-induced conformational transitions, such as chair–boat transitions of the pyranose rings^[12] and forced rotations of the hydroxymethyl group between various rotameric states.^[13]

We propose that similar to force-induced conformational transitions, the existence of intramolecular hydrogen bonds should be revealed directly by force spectroscopy by registering their effect on the molecular elasticity. To test this hypothesis we measured force spectrograms of amylose, a linear 1→4-linked α -D-glucan with the known propensity to form inter-residue H bonds,^[4,5] in various solvents. These solvents, by virtue of their widely different dielectric constants γ , were expected to either promote (low γ values) or inhibit (high γ values) the formation of intramolecular hydrogen bonds by controlling the electrostatic share of the bonding energy. Thus, by immersing amylose in solvents such as water ($\gamma = 80$) and dimethyl carbonate (DMC; $\gamma = 3.1$) we expected to control its hydrogen-bonding ability. The existence of H bonds could be then tested mechanically in single-molecule stretching measurements.

AFM stretching measurements were carried out on single amylose molecules in deionized water, dimethyl sulfoxide (DMSO, $\gamma = 47.2$), and dimethyl carbonate (DMC). The stretching of amylose in all these solvents is reversible (see the Supporting Information). Figure 1 compares typical force spectrograms of single amylose chains in these solvents. We recorded a total of 16 single-amylose force spectrograms in

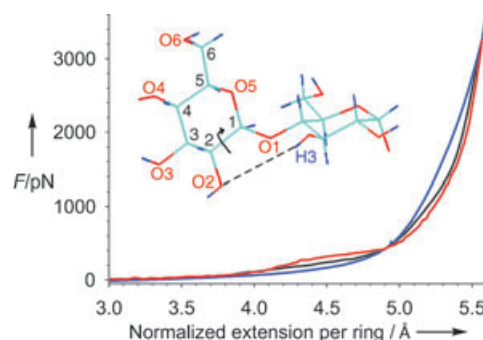


Figure 1. A comparison of typical force–extension relationships for amylose in H₂O (red trace), DMSO (black trace), and DMC (blue trace). The extensions were normalized by the molecules' length, measured at a common force of 3270 pN and then multiplied by the length of a single ring (O₄–O₁ distance) also determined at 3270 pN (see the Supporting Information). The inset shows the structure of maltose, a building block of amylose.

water, 11 in DMSO, and 11 in DMC, which displayed the same features as the respective spectrograms shown in Figure 1. From Figure 1 it is clear that the dielectric constant of the medium strongly affects the molecular elasticity of amylose. The difference between the recordings obtained in water and other solvents increases with the difference in their respective dielectric constants. The plateau feature, which is characteristic of the force spectrograms in water,^[12] disappears progressively in the media of lower dielectric constant, and the slope of the force extension curves at higher extensions (>5.0 Å per ring) increases abruptly relative to that determined in water. This behavior results in a crossover of the force–extension curves, which at low extensions (<4.8 Å per ring) run below and at high extensions (>5.0 Å per ring) above the trace obtained in water.

To clarify the effect of the dielectric constant of the medium on amylose elasticity we carried out molecular dynamics simulations of the stretching process using the steered molecular dynamics (SMD) protocol implemented in the program NAMD^[15] and a new CHARMM-based force field for carbohydrates.^[16] Similar SMD simulations performed on 1,6-linked glucans (pustulan and dextran), using the same force field, produced force–extension characteristics that agreed very well with our experimental AFM data.^[13] In SMD one terminal of the molecule is fixed and the other is pulled by a Hookean spring, thus simulating AFM stretching experiments. The simulations were carried out on a chain composed of ten glucopyranose rings, and we used the simplest implicit solvent model, in which the solvent is represented solely by the fixed dielectric constant, γ , which normalizes all the electrostatic interactions. We carried out two 200-ns SMD simulations for two extreme cases, with $\gamma = 80$ for water and $\gamma = 1$ for vacuum (Figure 2). We note that in both simulations the final conformation of the stretched pyranose rings is a skew boat (Figure 2 a, inset). However, the force–extension curves obtained from these simulations significantly differ in a way that is consistent with our experimental data. Similar to the force–extension curve obtained in DMC, the curve obtained from the vacuum SMD ($\gamma = 1$) shows no hint of the plateau feature. In addition,

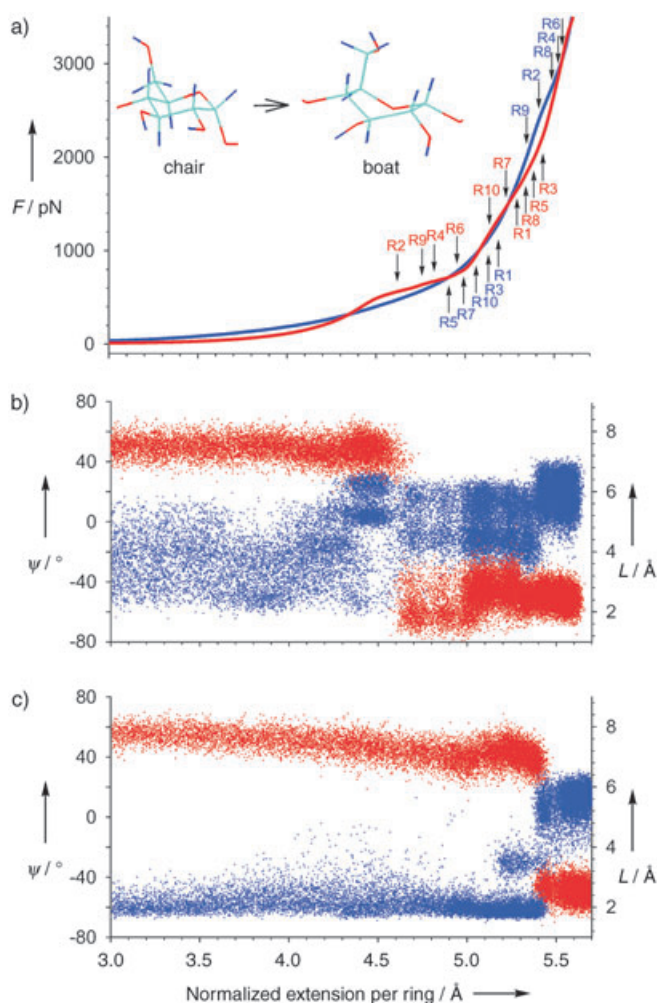


Figure 2. a) A comparison of force–extension curves of amylose obtained by 200-ns SMD simulations in water (red curve) and in vacuum (blue curve). The arrows indicate positions at which the individual rings flipped to a boatlike conformation. The inset shows the structures of the ring shortly before and after the conformational transition (generated using the program VMD^[19]). b) SMD trajectories of the O2–H3' distance (L) between rings 2 and 3 (blue trace, right axis) and of the ring dihedral angle $\psi = \text{O1–C1–C2–O2}$ (red trace, left axis) during the stretching process of amylose in water. c) Same as (b) but in a vacuum.

at intermediate extensions this curve runs under, and at higher extensions above, the curve obtained in the water SMD ($\gamma = 80$). Along the force–extension curves in Figure 2a we marked positions at which the individual rings underwent chair–boat transitions. It is evident that these transitions occurred later during the stretching in vacuum than in water, where 40 % of the rings flipped to a boatlike conformation during the plateau phase. Our SMD result obtained in implicit water is similar to the result obtained for amylose using the quantum mechanics based SMD method and explicit water, where 50–60 % of the rings changed their conformation during the plateau phase.^[17] We conclude that in vacuum the forced chair–boat transitions are shifted to higher forces and thus require a higher energy input compared to the transitions in water.

In Figure 2b and c we monitor the behavior of the putative O2–H3' hydrogen bonds (Figure 1, inset) between adjacent rings in water and in vacuum and analyze the trajectories of the ring conformation (dihedral angle $\psi = \text{O1–C1–C2–O2}$). In water (Figure 2b) the distance between O2 and H3' varies greatly and oscillates between 2 and 5 Å before the chair–boat transition and between 3.5 and 6.5 Å after the transition. The transition itself, monitored as an abrupt change in ψ occurs at the normalized extension of ≈ 4.6 Å per ring at a force of ≈ 500 pN. Clearly, the O2–H3' distance between the second and third pyranose rings, which is representative of other ring pairs as well, does not support a hydrogen bond between these rings.

In vacuum the O2–H3' distance (Figure 2c) covers a much smaller range, 1.7–2.4 Å, which is consistent with a fairly strong hydrogen bond between these rings. Ring 2 flips to a skew-boat conformation at the normalized extension of 5.4 Å per ring, corresponding to a force of ≈ 2300 pN, close to the end of the stretching cycle. During this transition there is an abrupt increase in the O2–H3' distance to ≈ 5 Å, which permanently breaks the hydrogen bond between these two rings. We conclude that in a medium of a low dielectric constant, strong hydrogen bonds between adjacent rings are formed in amylose, which involve the interaction between O2 and H3' atoms. These bonds mechanically link adjacent rings and rigidify the amylose backbone. They must be broken before the rings can flip to an extended, skew-boatlike conformation. As a result, chair–boat transitions occur on average at higher extensions and forces and from already highly deformed and extended chair conformations, in which the O1–O4 distance is significantly greater than that in a relaxed chair. Therefore these transitions contribute relatively less to the chain contour length than those that occur at low forces (as in water). This effect eliminates the plateau feature from the force–extension curve.

We note that although the final conformations of the stretched pyranose rings in water and vacuum are similar (skew-boat), the conformational pathways leading to these conformations are different. In the case of a vacuum (or a medium of low dielectric constant) the stretching process, in addition to reducing the configurational entropy of the chain and flipping the rings to a skew-boat conformation, also breaks the inter-residue hydrogen bonds that are not permanently formed in water. Thus by comparing the experimental force extension curves obtained in water and in a low-dielectric-constant medium, it should be possible to estimate the strength of these hydrogen bonds. This can be done by calculating and comparing the increase in the free energy of the amylose chain ΔG when stretched to the same extension L_{max} in water and in DMC. ΔG can be calculated as the reversible work of the stretching force [Eq. (1)] This work can

$$\Delta G = \int_0^{L_{\text{max}}} F dx \quad (1)$$

be measured by integrating the area under the force–extension curve. When the amylose extension x is normalized for one ring, as in Figure 1, ΔG represents the change in the

free energy per ring and $\Delta G_{\text{H bond}} = \Delta G_{\text{DMC}} - \Delta G_{\text{H}_2\text{O}}$ corresponds to the strength of the inter-residue hydrogen bond per ring (see the Supporting Information). We find that on average $\Delta G_{\text{H bond}}$ is $1.5 \text{ kcal mol}^{-1}$ (see the Supporting Information), which is a very reasonable estimate for the energy of a single hydrogen bond in maltose. Recently, Chen and Naidoo calculated the strength of this hydrogen bond in vacuum to be $4.99 \text{ kcal mol}^{-1}$.^[7] If we assume that this energy scales inversely with the dielectric constant of the medium, we arrive at a value of $1.61 \text{ kcal mol}^{-1}$ for DMC ($\gamma = 3.1$), which is very close to our estimate based on the AFM measurements.

Finally, if the interpretation of the results of our AFM measurements on amylose in terms of the hydrogen-bonding model is correct, eliminating the ability of amylose to form inter-residue H bonds altogether should make its elasticity solvent-independent. The ability to form H bonds can be abolished by replacing the hydroxy groups with the groups that cannot form H bonds, for example, acetates. In Figure 3

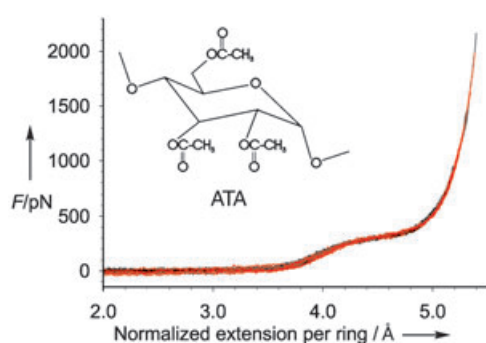


Figure 3. A comparison of AFM-determined force spectrograms of ATA in water (red curves, five different recordings) and in DMC (black traces, five different curves). The inset shows the structure of the ATA monomer.

we show the force–extension curves obtained by stretching single amylose triacetate (ATA)^[18] molecules in water and in DMC. It is now clear that there is no difference between the recordings for ATA obtained in media of high and low dielectric constants, which corroborates our original conjecture. Moreover, all of the ATA curves (in DMC and water) look similar to the curves obtained on native amylose in water. This result suggests that: 1) water effectively eliminates inter-residue H bonds of amylose; 2) the acetate substituents do not affect the elasticity of amylose other than by eliminating H bonds; and 3) once the possibility to form inter-residue H bonds has been eliminated, the solvents play no significant role in amylose elasticity. The last conclusion also implies that the contributions to the force–extension relationship from changes in the interglycosidic torsion angles that accompany amylose stretching are similar in water and in DMC and therefore cannot explain the differences in the elasticity of native amylose observed in these solvents.

In conclusion, amylose can form strong inter-residue hydrogen bonds, which significantly rigidify the polymer, in solvents with a low dielectric constant. However, these H bonds are effectively eliminated in water. Single-molecule

force spectroscopy is an ideal method for directly examining the hydrogen bonding in polysaccharides and accurately measuring their strength under various solvent conditions. The strength of our approach is in that once solubilized and adsorbed to a substrate, polysaccharides can be examined by AFM in a variety of solvents, including those they normally “do not like”, because the AFM tip pulls the molecules into these solvents. As polysaccharide structures and functions are greatly affected by extensive networks of intra- and inter-molecular hydrogen bonds, our method to directly detect and examine such bonds may find widespread application in the carbohydrate research and beyond.

Experimental Section

Force spectroscopy measurements on amylose were carried out in a PicoForce AFM (Veeco Metrology Group, Santa Barbara, CA) and a home-built force spectrometer.^[12] Amylose (type III, from potato; Sigma-Aldrich) was dissolved in water at a concentration of 0.001–0.1 % (w/v) by heating ($\approx 90^\circ\text{C}$). A layer of polysaccharide molecules was created by drying a drop of these solutions onto glass coverslips, which had been cleaned by boiling in HCl and then in H_2O_2 . Then the dehydrated sample was rinsed extensively with water to leave only those molecules that were tightly adsorbed to the glass surface.^[14] After the substrate had been thoroughly dried and placed in the AFM, the liquid chamber was filled with an appropriate solvent for pulling measurements. To pick up amylose molecules, an AFM tip (Si_3N_4 ; Veeco) was pressed down onto the sample for 1–3 s at forces of 1–20 nN. Frequently, no molecule adhered to the tip, and no force extension curve (force spectrogram) was recorded in such a case. Occasionally, several molecules with various lengths adhered simultaneously to the tip, and a complicated force–extension pattern was recorded with several overlapping and irregular force peaks, which correspond to simultaneous stretching and sequential detachment of these molecules. Such recordings are difficult to interpret and are not included in this communication (see the Supporting Information). However, in $\approx 10\%$ of the recordings a quite distinct pattern, which can be attributed to individual amylose molecules, was registered. The unmistakable features of these single-amylose force spectrograms are: the characteristic plateau that always appears at a force of $\approx 270 \text{ pN}$ in H_2O , full reversibility of the stretching process (forward and backward stretching traces are identical), and the overlapping of all the recordings after they have been normalized to a common extension (see the Supporting Information). The normalization procedure is important as it allows the comparison of force spectrograms obtained on molecular fragments that vary in length. This is a common procedure in AFM-based force spectroscopy, because AFM tip randomly picks up polymer fragments to be stretched (see the Supporting Information).^[8,20]

Received: September 22, 2004

Revised: October 19, 2004

Published online: March 22, 2005

Keywords: carbohydrates · hydrogen bonding · molecular dynamics · scanning probe microscopy · solvent effects

[1] G. Gemmecker, *Angew. Chem.* **2000**, *112*, 1276–1279; *Angew. Chem. Int. Ed.* **2000**, *39*, 1224–1226.

[2] V. S. R. Rao, P. K. Qasba, P. V. Balaji, R. Chandrasekaran, *Conformation of Carbohydrates*, Amsterdam, Harwood Academic, **1998**.

- [3] a) Y. Nishiyama, J. Sugiyama, H. Chanzy, P. Langan, *J. Am. Chem. Soc.* **2003**, *125*, 14300–14306; b) M. Jarvis, *Nature* **2003**, *426*, 611–612.
- [4] M. E. Gress, G. A. Jeffrey, *Acta Crystallogr. Sect. B* **1977**, *33*, 2490–2495.
- [5] a) F. Takusagawa, R. A. Jacobson, *Acta Crystallogr. Sect. B* **1978**, *34*, 213–218; b) I. Tanaka, N. Tanaka, T. Ashida, M. Kakudo, *Acta Crystallogr. Sect. B* **1976**, *32*, 155–160; c) F. Brisse, R. H. Marchessault, S. Perez, P. Zugenmaier, *J. Am. Chem. Soc.* **1982**, *104*, 7470–7476; d) K. Gessler, I. Uson, T. Takata, N. Krauss, S. M. Smith, S. Okada, G. M. Sheldrick, W. Saenger, *Proc. Natl. Acad. Sci. USA* **1999**, *96*, 4246–4251.
- [6] a) A. D. French, D. P. Miller, *ACS Symp. Ser.* **1994**, *569*, 235; b) S. Mendonca, G. P. Johnson, A. D. French, R. A. Laine, *J. Phys. Chem. A* **2002**, *106*, 4115–4124; c) R. A. Klein, *J. Am. Chem. Soc.* **2002**, *124*, 13931–13937; d) F. A. Momany, J. L. Willett, *J. Comput. Chem.* **2000**, *21*, 1204–1219; e) F. A. Momany, J. L. Willett, *Carbohydr. Res.* **2000**, *326*, 210–226; f) K. N. Kirschner, R. J. Woods, *Proc. Natl. Acad. Sci. USA* **2001**, *98*, 10541–10545; g) J. W. Brady, R. K. Schmidt, *J. Phys. Chem.* **1993**, *97*, 958–966; h) K. J. Naidoo, M. Kuttel, *J. Comput. Chem.* **2001**, *22*, 445–456.
- [7] J. Y.-J. Chen, K. J. Naidoo, *J. Phys. Chem. B* **2003**, *107*, 9558–9566.
- [8] a) M. Rief, F. Oesterhelt, B. Heymann, H. E. Gaub, *Science* **1997**, *275*, 1295–1297; b) M. Grandbois, M. Beyer, M. Rief, H. Clausen-Schaumann, H. E. Gaub, *Science* **1999**, *283*, 1727–1730.
- [9] F. Oesterhelt, M. Rief, H. E. Gaub, *New J. Phys.* **1999**, *1*, 6.1–6.11.
- [10] P. E. Marszalek, H. Lu, H. Li, M. Carrion-Vazquez, A. F. Oberhauser, K. Schulten, J. M. Fernandez, *Nature* **1999**, *402*, 100–103.
- [11] P. J. Flory, *Principles of Polymer Chemistry*, Cornell University Press, **1953**.
- [12] a) P. E. Marszalek, A. F. Oberhauser, Y.-P. Pang, J. M. Fernandez, *Nature* **1998**, *396*, 661–664; b) P. E. Marszalek, Y.-P. Pang, H. Li, J. E. Yazal, A. F. Oberhauser, J. M. Fernandez, *Proc. Natl. Acad. Sci. USA* **1999**, *96*, 7894–7898; c) P. E. Marszalek, H. Li, A. F. Oberhauser, J. M. Fernandez, *Proc. Natl. Acad. Sci. USA* **2002**, *99*, 4278–4283.
- [13] a) G. Lee, W. Nowak, J. Jaroniec, Q. Zhang, P. Marszalek, *Biophys. J.* **2004**, *87*, 1456–1465; b) G. Lee, W. Nowak, J. Jaroniec, Q. Zhang, P. Marszalek, *J. Am. Chem. Soc.* **2004**, *126*, 6218–6219.
- [14] H. Li, M. Rief, F. Oesterhelt, H. E. Gaub, *Adv. Mater.* **1998**, *10*, 316–319.
- [15] L. Kalé, R. Skeel, M. Bhandarkar, R. Brunner, A. Gursoy, N. Krawetz, J. Phillips, A. Shinozaki, K. Varadarajan, K. Schulten, *J. Comput. Phys.* **1999**, *151*, 283–312.
- [16] M. Kuttel, J. W. Brady, K. J. Naidoo, *J. Comput. Chem.* **2002**, *23*, 1236–1243.
- [17] Z. Lu, W. Nowak, G. Lee, P. E. Marszalek, W. Yang, *J. Am. Chem. Soc.* **2004**, *126*, 9033–9041.
- [18] Y. Takahashi, S. Nishikawa, *Macromolecules* **2003**, *36*, 8656–8661.
- [19] W. Humphrey, A. Dalke, K. Schulten, *J. Mol. Graphics* **1996**, *14*, 33–38.
- [20] P. E. Marszalek, H. Li, J. M. Fernandez, *Nat. Biotechnol.* **2001**, *19*, 258–262.